ELSEVIER

Journal of Organometallic Chemistry 486 (1995) 95–104

Journal of Organometallic Chemistry

Electrochemical reduction of 1,10-bis(1-phenyl-3-methyl-5-hydroxy-4-pyrazolyl)-1,10-decanedione. Characterization of its electrogenerated mononuclear Co^{II}, Ni^{II} and Cu^{II} complexes. ESR properties of Co^{II} and Cu^{II} complexes

Alain Louati [a,*], Agus Kuncaka [a], Maurice Gross [a,*], Catherine Haubtmann [b], Maxime Bernard [b], Jean-Jacques André [b,*], Jean-Pierre Brunette [c]

[a] *Laboratoire d'Electrochimie et de Chimie Physique du Corps Solide, URA au CNRS no. 405, Université Louis Pasteur, 4 rue Blaise Pascal, F-67000 Strasbourg, France*

[b] *Institut Charles Sadron (UP au CNRS no. 0022, Université Louis Pasteur), 6 rue Boussingault, F-67083 Strasbourg, France*

[c] *Laboratoire de Chimie Minérale, URA au CNRS no. 405, Ecole Européenne des Hautes Etudes des Industries Chimiques de Strasbourg, 1 rue Blaise Pascal, F-67008 Strasbourg, France*

Received 6 April 1994

Abstract

The reductive electrochemistry of 1,10-bis(1-phenyl-3-methyl-5-hydroxy-4-pyrazolyl)-1,10-decanedione (H_2L^3 = **3**) in tetrahydrofuran on a mercury electrode is reported. Voltammetric, polarographic, coulometric and spectroscopic data indicate that **3** undergoes an irreversible two-electron reduction, generating a transient species that may involve the carbonyl groups. This step is followed by a rapid chemical reaction that produces the stable dianion $(L^3)^{2-}$. The electrochemically generated dianion reacts with M^{II} trifluoromethanesulfonate to afford the corresponding (1/1) complexes $[Co^{II}L^3]$, $[Ni^{II}L^3]$ and $[Cu^{II}L^3]$ respectively. These complexes have been characterized by spectroscopic (UV-Vis, IR and mass spectroscopies) and electrochemical (polarography) techniques. ESR studies were carried out on the Co^{II} and the Cu^{II} complexes. Determination of the environment of the Co^{II} and Cu^{II} ions in each complex was attempted using all the experimental results. $[Co^{II}L^3]$ is high-spin with a distorted octahedral geometry and $[Cu^{II}L^3]$ has a tetrahedrally distorted square-planar symmetry.

Keywords: Electrochemistry; Copper; Cobalt; Nickel; Pyrazoline complexes; EPR

1. Introduction

We have recently reported [1] results on the electrochemically-promoted generation of mononuclear copper complexes $[Cu^{II}L^1]$ and $[Cu^{II}L^2]$. This complexation proceeds as addition of copper(II) salt to a solution of $(L^1)^{2-}$ and $(L^2)^{2-}$ resulting from exhaustive electroreductions of the bis(β-diketones) H_2L^1 = **1** and H_2L^2 = **2**.

In this paper, we report the extension of this study to the electrogeneration of transition metal complexes through direct electrochemical reduction of 1,10-bis(1-phenyl-3-methyl-5-hydroxy-4-pyrazolyl)-1,10-decanedione, H_2L^3 (**3**).

Substituted pyrazolones, the parent compounds of substituted β-diketones, have been employed in a number of solvent extraction studies [2–4] but no electrochemical studies have been published. The electrochemical reduction of **3** is presented in detail in this paper. Future studies will report the electrochemical properties of additional pyrazolones. **3** was chosen to allow comparison with **1** and **2**, and to study in particular the effect of the simultaneous presence of acetyl and of pyrazolone moieties, on (i) their electrochemical behaviour, and on (ii) the mechanism of the electro-

* Corresponding authors.

SSDI 0022-328X(94)05022-4

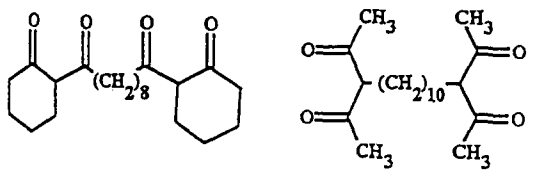

H_2L^1, = 1 H_2L^2, = 2

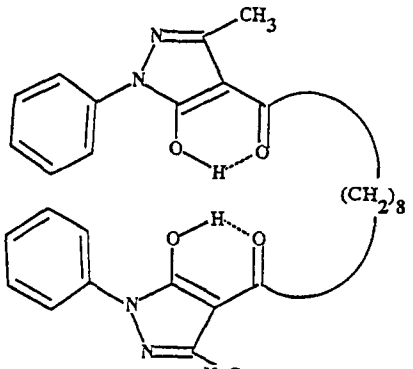

H_2L^3, = 3

chemically-promoted generation of metal(II) complexes.

2. Experimental section

2.1. Materials

Tetrahydrofuran (THF, Fluka) was distilled from sodium/benzophenone and, just before use, from CaH_2. All other solvents were dried using standard methods and distilled prior to use. Tetrabutylammonium perchlorate (TBAP, Fluka) used as supporting electrolyte was recrystallized from ethanol/water (60/40) and dried under vacuum at 70°C for 48 h. CAUTION! Perchlorate salts are dangerous and should be handled with care.

1,10-bis(1-phenyl-3-methyl-5-hydroxy-4-pyrazolyl)-1,10-decanedione was prepared by Jensen's method [5] and recrystallized three times from a chloroform-ethanol mixture.

2.2. Physical measurements

IR spectra were recorded on a Bruker FT-IR IFS 66 spectrometer. UV-visible absorption spectra were obtained with a Shimadzu UV 260 spectrometer. The mass spectra were recorded on a TSQ70 (Finnigan MAT) spectrometer. Microanalyses of C, H and N elements were carried out on an EA1108 Elemental Analyzer (Carlo Erba). ESR experiments were performed using a Bruker ESP300 X-band spectrometer provided with a TE_{102} cavity and coupled to a HP9000-360 computer for initial condition setting and data acquisition. An Oxford ESR900 cryostat was used for low-temperature characterization.

2.3. Electrochemistry

Electrochemical measurements were made on tetrahydrofuran solutions containing TBAP as supporting electrolyte. A solvent-saturated argon purge and a three-electrode configuration were used throughout. Potentials are referenced to a saturated calomel electrode (SCE), which was isolated from the working compartment electrode with a $[Bu_4N]ClO_4$–THF salt bridge. Cyclic voltammetric and polarographic measurements were performed with a multipurpose PRG4 device (SOLEA-Tacussel) equipped with a current sampling system which makes it possible to carry out cyclic voltammetry with a dropping mercury electrode (DME) as the working electrode. A platinum wire was employed as the counter-electrode. Controlled-potential bulk electrolysis experiments were carried out in a two-compartment cell using a stirred mercury-pool as the working electrode. The working potentials were controlled by a PRT 100 potentiostat (SOLEA-Tacussel).

2.4. Electrogeneration of metal complexes

$[M^{II}L^3]$ (M = Co, Ni or Cu). The general procedure involved first the exhaustive reduction of **3** (2 Faraday/mol) at constant potential (−2.4 V), followed by addition of the metal(II) salts (Scheme 1).

2.5. Preparation of the cobalt(II) complex: $[CoL^3]$

After exhaustive electrolysis at −2.4 V of **3** (50 mg, 0.097 mmol) in THF + 0.2 M TBAP, cobalt(II) trifluoromethanesulfonate (52 mg, 0.145 mmol) was added to the yellow solution. The resulting red-orange solution was then separated from mercury and evaporated to dryness under reduced pressure. The residue was then treated with toluene, in which TBAP is insoluble, and filtered. The solution was concentrated and purified by chromatography over silica gel using 10% toluene in THF to afford a pale brown product (23 mg, 0.040 mmol, 41%).

2.6. Preparation of the nickel(II) complex: $[NiL^3]$

A solution of **3** (50 mg, 0.097 mmol) in THF + 0.2 M TBAP was completely reduced at −2.4 V producing a yellow solution. To this solution, nickel(II) trifluoromethanesulfonate (34.5 mg, 0.097 mmol) was added.

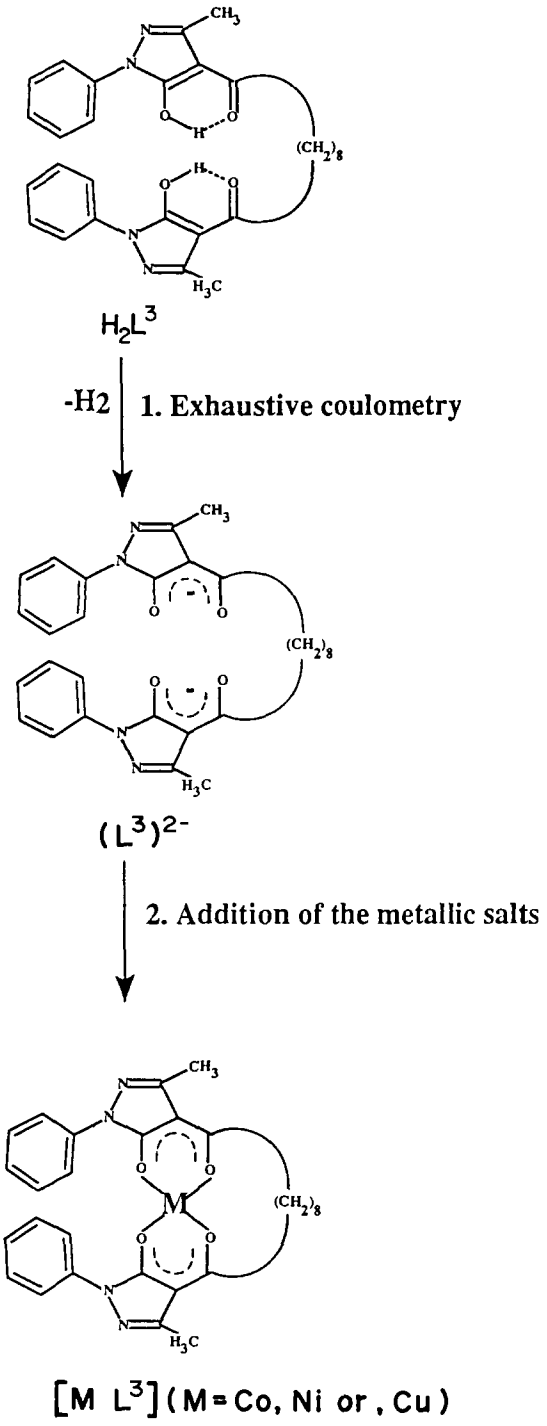

Scheme 1.

The resulting green solution was separated from mercury and then evaporated to dryness under reduced pressure. The residual solid was shaken with toluene to separate the insoluble TBAP from the soluble complex. The filtered solution was then evaporated to dryness and dried several hours under vacuum at 50°C to yield 38.6 mg (0.068 mmol, 70%) of a yellow-green powder.

2.7. Preparation of the copper(II) complex: [CuL^3]

The copper complex was prepared by addition of copper(II) trifluoromethanesulfonate (35.14 mg, 0.097 mmol) to a yellow solution produced by bulk reduction of **3** (50 mg, 0.097 mmol) in THF + 0.2 M TBAP at −2.4 V. After removing the mercury, the solution was evaporated to dryness under reduced pressure. The residual solid was washed several times with dry acetone, filtered, and dried under vacuum to yield 46.9 mg (0.081 mmol, 83%) of a blue-green powder.

3. Results and discussion

3.1. Electrochemical reduction of 3

3.1.1. Polarography

A polarogram of the reduction of **3** ($5 \cdot 10^{-4}$ mol dm^{-3}) in 0.1 mol dm^{-3} TBAP in THF at a DME is given in Fig. 1. Two cathodic waves were observed in the potential range +0.5 to −3.0 V. The first wave at −1.80 V was well defined, but the second wave was not so clear. For this second wave $E_{1/2} = -2.25$ V was obtained by differential pulse polarography. Furthermore, the height of the second wave was markedly smaller than that of the first. Considering the results obtained earlier for the reduction of **1** and **2**, it seemed unlikely that the second wave of **3** was due to reduction of the radical anion owing to its very low limiting current. **1** exhibited only a single irreversible two-electron reduction wave while two successive reduction waves with equal limiting currents were observed for **2**

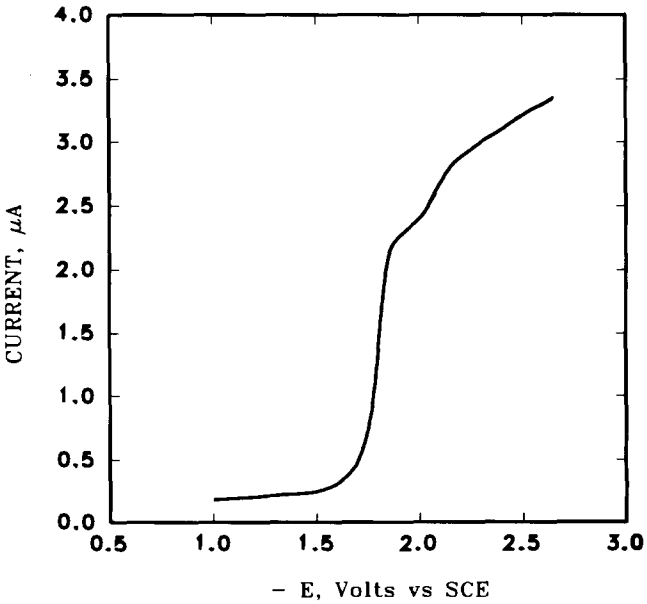

Fig. 1. Polarogram of $5 \cdot 10^{-4}$ mol dm^{-3} **3** in THF + 0.1 mol dm^{-3} TBAP at a dropping mercury electrode.

under the same conditions [1]. Assuming similar diffusion coefficients of **3** and **1**, the comparison of the limiting current of **3** with that of an equimolar solution of **1** indicated that the first reduction wave of **3** corresponded to the uptake of two electrons. This was further confirmed by coulometric results. A log plot of this wave [E vs. $\log(I_{lim}/I_{lim} - I)$] was nearly linear with a slope of −85 mV/log indicating an irreversible two-electron reduction. A slope of −60 mV/log is expected for a reversible two-electron transfer involving two non-interacting sites [6]. The slope of −0.51 for the linear plot of log I_{corr} vs. log t_{pol} indicated that the reduction process of **3** was not limited only by diffusion, but that chemical reaction(s) were also involved [7]. It was therefore reasonable to assume that the second wave was due to the reduction of an electroactive species generated by the chemical reaction(s) following the first electron-transfer of **3**. This first electron-transfer, which may be ascribed to the carbonyl groups, occurred at a potential ca. 500 mV more anodic than for **1** and **2**. This anodic shift probably reflects the electron-withdrawing effect of the pyrazolone groups in **3**.

3.1.2. Cyclic voltammetry

Fig. 2 illustrates the changes in the cyclic voltammograms at different scan rates between −1.0 and −3.0 V. At low scan rates ($v \leq 5$ V s^{-1}), the cyclic voltammograms (Fig. 2a) exhibited a well-defined reduction peak at −1.90 V (process 1) and a poorly-defined reduction peak (process 2) of much lower intensity at a more negative potential. Both reduction processes were irreversible on this time scale, as demonstrated by the absence of coupled reoxidation peaks on the back scan. When the scan rate was increased ($v > 5$ V s^{-1}), a broad anodic wave (process 3) appeared. The intensity of this reoxidation current was enhanced as the scan rate increased while at the same time the height of peak 2 decreased. At high scan rates ($v = 50$ V s^{-1}, Fig. 2b), the second reduction peak (process 2) vanished and only the first peak remained. The characteristics (current and potential) of this first peak were studied over the scan-rate range 2–100 V s^{-1}. At low scan rates ($v \leq 5$ V s^{-1}) a linear relationship was observed between the peak current and $v^{1/2}$, but this linear relationship was not obeyed beyond 10 V s^{-1}, when $Ip/v^{1/2}$ decreased. Thus the ohmic drop was considered negligible only up to the scan rate 10 V s^{-1}. However, the peak potential (E_{pc}) vs. log v was linear at all scan rates. Cyclic voltammograms were also obtained at low-temperature for the reduction of **3**. As shown in Fig. 3, the second peak current disappeared at ca. −5°C. These results were consistent with those from polarography, indicating that the first reduction was irreversible and involved an electron-transfer reaction followed by a chemical step [8].

3.1.3. Coulometric reduction and characterization of the generated species

Controlled potential electrolysis of a solution of **3** in THF – $[Bu_4N]ClO_4$ at −2.0 V produced a yellow solution of reduced pyrazolone with consumption of 1.75 electrons per molecule. The cathodic scan of the resulting solution showed that the second wave remained observable and that a new oxidation wave appeared at 0.25 V. When the electrolysis was continued at the potential of the second cathodic wave, −2.4 V, ca. 0.2 more of an electron was consumed per molecule of **3**. The cathodic scan of the resulting solution showed the disappearance of both reduction signals of **3**, while the limiting current of the oxidation wave ($E_{1/2} = 0.25$ V) increased. Finally, when exhaustive coulometry of **3** was carried out at the plateau

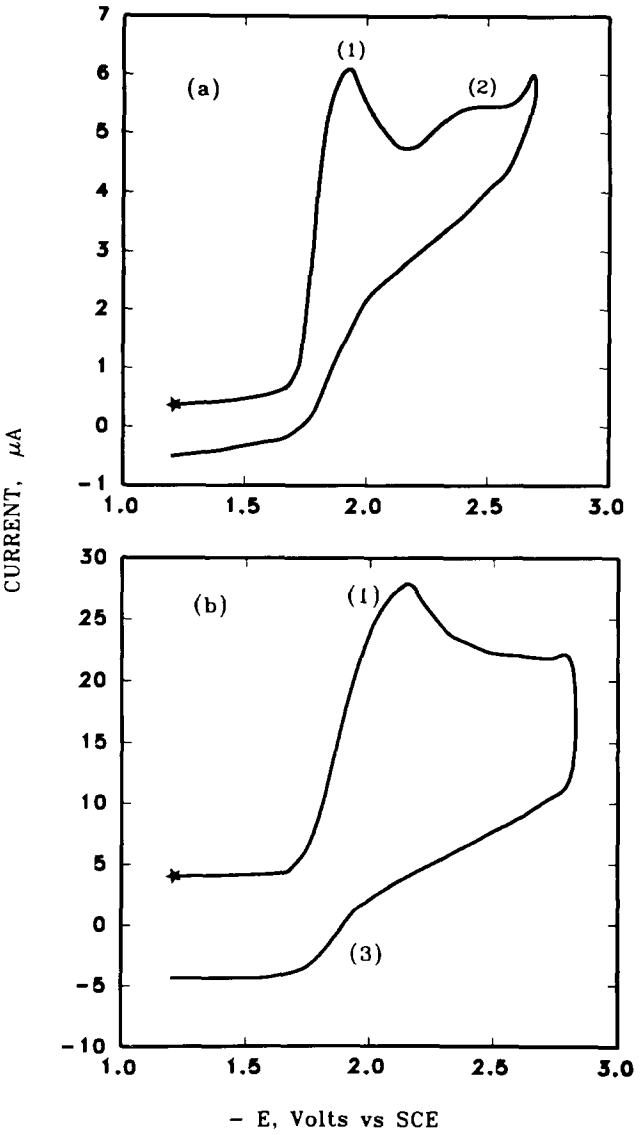

Fig. 2. Cyclic voltammograms of $5 \cdot 10^{-4}$ mol dm^{-3} **3** in THF+0.1 mol dm^{-3} TBAP. The scan rates are (a) 5 V s^{-1}, (b) 50 V s^{-1} at room temperature. * denotes start of the scan.

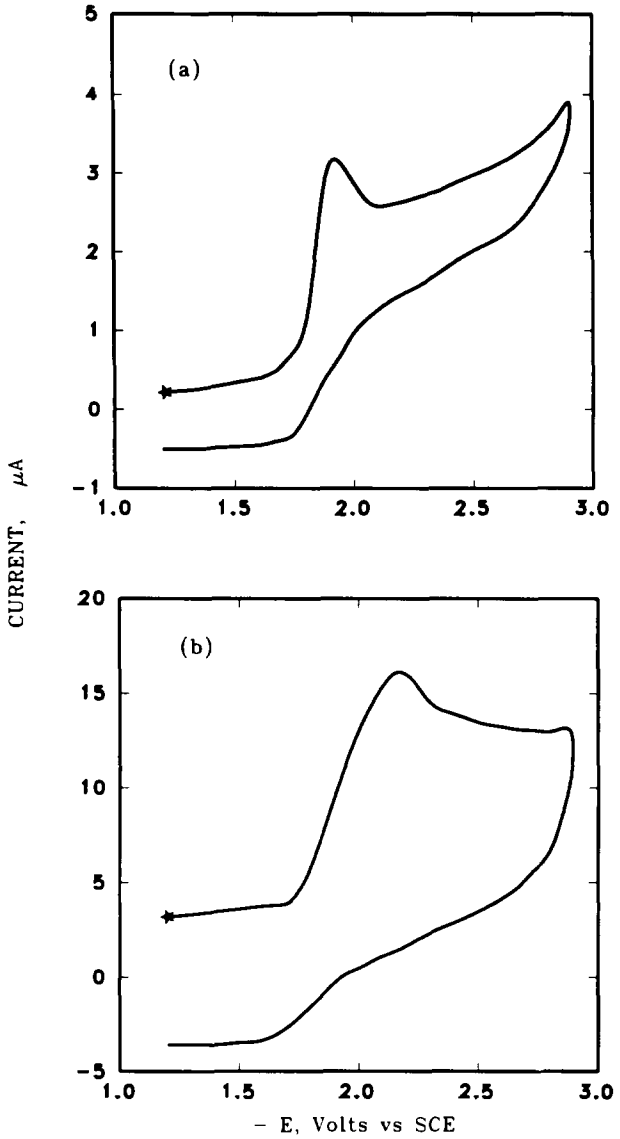

Fig. 3. Cyclic voltammograms of $5 \cdot 10^{-4}$ mol dm^{-3} **3** in THF+0.1 mol dm^{-3} TBAP at −5°C; scan rates (a) 5 V s^{-1}, (b) 50 V s^{-1}. ⋆ denotes start of the scan.

potential of the second reduction wave ($E_{app.}$ = −2.4 V), the number of electrons exchanged (n) was close to 2 (1.85). In all cases, plots of ln i vs. t were not linear, thus confirming that the reduction of **3** involved an irreversible chemical reaction following the charge transfer. These results confirm those reported above from voltammetry.

The solution obtained after the exhaustive two-electron reduction of **3** was examined by UV-visible spectroscopy in the 200–500 nm range. The final electrogenerated species exhibited a well-defined absorption band at 260 nm and a shoulder at 285 nm, an interchange of the absorption bands and an approximate 20 nm red shift when compared to the unreduced **3** (λ_{max} (nm): 240sh and 265). This latter result fits well with the literature data [9] on pentandionate systems and it indicates that the final species in the reduced solution of **3** is the anionic species $(L^3)^{2-}$.

On the basis of the above electrochemical and spectral data and the results obtained for **1** and **2**, it is proposed that the reduction of the carbonyl groups in **3** occurs in a reaction sequence involving a two-electron transfer followed by an irreversible chemical reaction ultimately leading to the bis(β-enolate) species $(L^3)^{2-}$. This is illustrated by the overall equation

$$H_2L^3 + 2e^- \longrightarrow \left\{(H_2L^3)^{2-}\right\}^* \longrightarrow (L^3)^{2-} + H_2$$

* not observed on the electrochemical measurements time scale.

The formation of $(L^3)^{2-}$ was promoted by the electrochemically generated unstable anionic base "$(H_2L^3)^{2-}$" and did not result from a dissociative reaction such as $H_2L^3 \rightarrow (L^3)^{2-} + 2H^+$. Such a reaction is highly unlikely in THF due to the weak acidic character of **3** (pKa ~ 5) [3]. Another clear indication was that the UV-visible spectra of the solutions did not show the presence of bis(β-enolate) species before the electrochemical reduction of **3**.

The above global reaction is very similar to that observed in the reduction of other β-diketones [10,11].

3.1.4. Electrochemical generation of bis(heterocyclic β-diketonato) mononuclear complexes: $[M^{II}L^3]$ (M = Co, Ni, or Cu)

An interesting and significant aspect of the above results was that the two-electron reduction of **3** ultimately generated $(L^3)^{2-}$. Based on this result, the feasibility of the direct preparation of transition metal complexes of cobalt(II), nickel(II) and copper(II) from solutions of $(L^3)^{2-}$ was explored.

The operation involved, first, the exhaustive reduction of **3** (2 Faraday/mol) at constant potential (−2.4 V), and, second, the addition of metal(II) salts. The resulting solutions were analyzed by polarography. The polarograms recorded after stoichiometric additions of copper(II) and nickel(II) trifluoromethanesulfonates show that the characteristic oxidation wave of $(L^3)^{2-}$ (Fig. 4a) disappeared, and a reduction wave appeared at −0.6 V (Fig. 4b) in the case of copper ($E_{1/2}$(uncomplexed Cu^{2+}) = 0.27 V) and at −1.81 V (Fig. 4c) in the case of nickel ($E_{1/2}$(uncomplexed Ni^{2+}) = −0.85 V). The situation was somewhat different with cobalt, for which the characteristic oxidation wave of $(L^3)^{2-}$ disappeared only upon addition of 1.5 equiv of Co^{2+}. In this case, the polarogram of the resulting solution exhibited two closely-spaced waves whose half potentials were −2.10 and −2.30 V, respectively, ($E_{1/2}$(uncomplexed Co^{2+}) = −0.99 V) as determined by differential pulse polarography (Fig. 5).

Comparison of the above $E_{1/2}$ values with those of several other bis(β-diketonato) transition metal com-

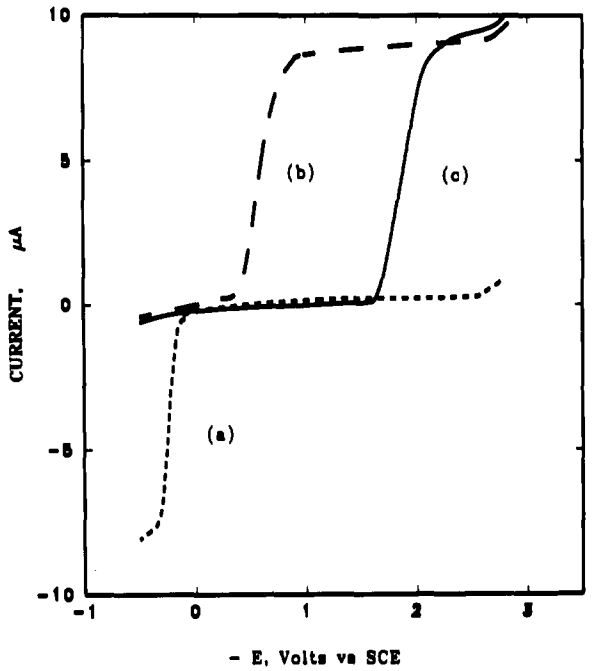

Fig. 4. Voltammetric illustration of M^{II} complexation by $(L^3)^{2-}$ (10^{-3} mol dm^{-3}) in THF + 0.1 mol dm^{-3} TBAP at a mercury electrode. D.c. polarograms: (a) after reductive electrolysis of **3** at −2.4 V; (b) after addition of Cu^{II} trifluoromethanesulfonate; (c) after addition of Ni^{II} trifluoromethanesulfonate; stoichiometry $M:L^3 = 1:1$.

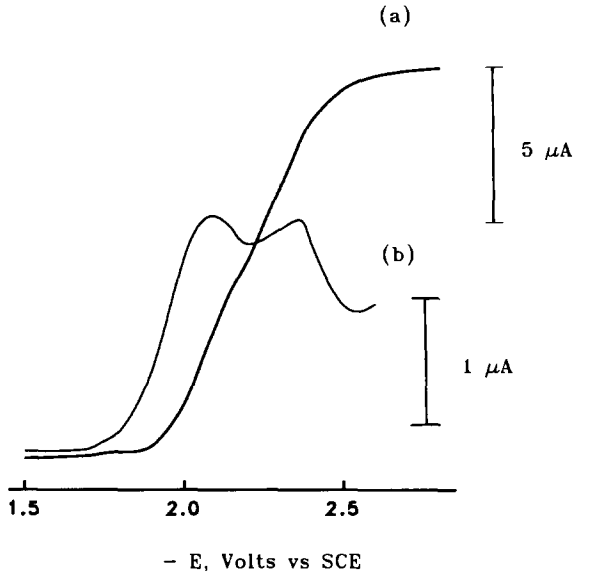

Fig. 5. Voltammetric illustration of Co^{II} complexation by $(L^3)^{2-}$ (10^{-3} mol dm^{-3}) in THF + 0.1 M TBAP: (a) D.c. polarogram and (b) differential pulsed polarogram (drop time 1 s; scan rate 5 mV s^{-1}; ramp 50 mV; polarization delay 0.95 s; potential pulse duration 40 ms; duration of each measurement 4 ms), after addition of Co^{II} trifluoromethanesulfonate (stoichiometry $Co^{II}:L^3 = 1.5:1$).

plexes, strongly suggested that the reduction of **3** followed by addition of M^{II} cations led to cobalt, nickel and copper complexes. These complexes have been isolated and characterized by elemental analysis and spectroscopic studies. The results are summarized in Table 1.

Considering the UV-Vis and IR spectral data in Table 1, the following comments may be made.

3.2. Electronic spectra

In all cases, chloroform solutions of the complexes exhibited absorption spectra consisting of a relatively weak broad band, ordinarily assigned to a d–d* transition, in the 620 to 660 nm range, two absorption signals

Table 1
Analytical, IR and UV-Vis data of metal(II) complexes of Co, Ni, or Cu

Compound	Analysis (%) [a]			ν(OH ··· O) [b] (cm^{-1})	ν(CO) [b] (cm^{-1})	ν(C ··· C) [b] (cm^{-1})	ν(M–O) [b] (cm^{-1})	λ [c]/nm	log ε [c]
	C	H	N						
H_2L^3	70.20(70.02)	6.90(6.65)	10.98(10.88)	2700	1630	1504		240sh	
						1495		260	4.46
						1492			
$[CoL^3]$	62.94(63.40)	5.59(5.66)	9.79(9.67)		1624	1506	510	248	4.72
								290sh	–
								416	3.37
								654	1.3
$[NiL^3]$	63.08(63.20)	5.61(5.73)	9.81(9.69)		1616	1506	511	264	4.76
						1495		~ 300sh	–
								472	1.69
								660	0.70
$[CuL^3]$	62.50(63.00)	5.56(5.90)	9.72(9.60)		1604	1490	511	253	4.69
							472	282sh	–
								620	1.43

[a] Calculated values in parentheses.
[b] Measured in KBr pellets.
[c] Measured in chloroform at room temperature.

which are attributed to $\pi-\pi^*$ transitions within a ligand molecule and a metal-to-ligand charge-transfer in the UV region. Comparison of these results with those reported for M^{II}-4-acyl-pyrazolone-5 and M^{II}-substituted-β-diketone chelates complexes [12,13] confirmed the formation of the M^{II} complexes with $(L^3)^{2-}$. The spectrum of the Co^{II} complex in particular showed several weak bands in the 510–602 nm range resembling those reported [14] for planar bis(acetylacetonato)cobalt(II) in chloroform. The absorption band at 472 nm for the [NiL^3] complex indicated that this complex probably has a square-planar geometry. The spectra of the square-planar nickel(II) chelates usually display an absorption band in the 400–500 nm range [15].

3.3. IR spectra

IR spectra (in a KBr disk) of all electrogenerated complexes were very similar and resemble those of both 1-phenyl-3-methyl-4-benzoyl-pyrazolone-5 complexes and 1-phenyl-3-methyl-4-acetyl-pyrazolone-5 complexes [12,16], and the chelates of β-diketones [17,18]. The intense broad OH $\cdots$ O band at 2700 cm^{-1} in the H_2L^3 spectrum was absent in the spectra of the complexes, indicating the absence of OH, as expected. The ligand band at 1630 cm^{-1}, assigned to C=O vibrations, was shifted to higher energy (6, 14 and 26 cm^{-1}) in the complexes, suggesting that C=O is involved in metal coordination. All complexes exhibit weak bands between 472 and 511 cm^{-1} characteristic of the metal–oxygen stretching frequency. The absence of band in the 3100–3500 cm^{-1} region indicated that the complexes were not solvated.

In each case positive chemical ionization spectrometry (CI) revealed molecular ion peaks at m/z = 572.2, 571.2, 575.1 and 577.2 corresponding to $[CoL^3]^+$, $[NiL^3]^+$, $[^{63}CuL^3]^+$ and $[^{65}CuL^3]^+$, respectively. This, together with UV-Vis, IR and microanalytical data (Table 1), suggested that the [ML^3] species were monomeric.

3.4. ESR properties of Cu^{II} and Co^{II} complexes

3.4.1. [CuL^3]

The spectrum of the copper complex diluted in chloroform recorded at 120 K and 47 mW incident power is illustrated in Fig. 6. Three species can be identified from the spectrum. Signals A and B correspond to a monomeric copper compound with nearly axial symmetry, B and A arising from the ^{65}Cu and ^{63}Cu isotopes respectively. Relative intensities on the low field side match the 2/3 (signal A) 1/3 (signal B) ratio. Hyperfine structure from the I = 3/2 copper atom was clearly detected and led to the following magnetic parameters for the ^{63}Cu A species: $g_\perp$ =

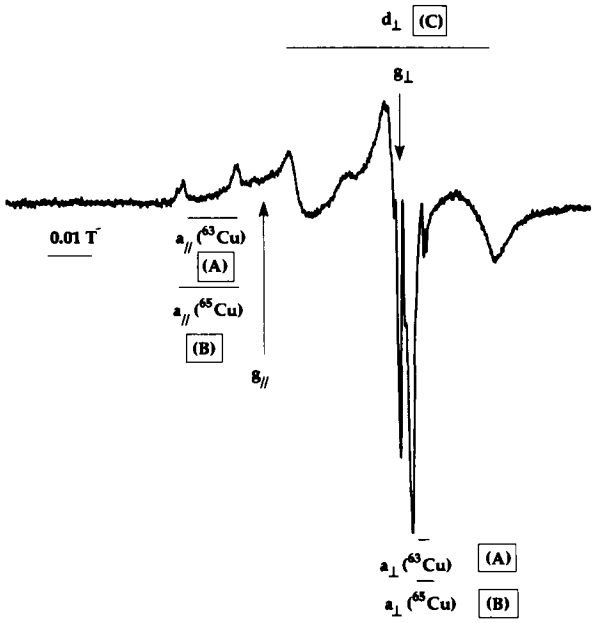

Fig. 6. ESR spectrum of the copper(II) complex in chloroform taken at 120 K and 47 mW incident power.

2.047, $g_\parallel = 2.324$, $a_\parallel = 135.7 \cdot 10^{-4}$, $a_\perp = 27.0 \cdot 10^{-4}$ cm^{-1}.

These values situate this monomeric complex at the border of the well-known Peisach-Blumberg diagrams [19] of $a_\parallel$ vs. $g_\parallel$ and a_{iso} vs. g_{iso} for O_4 ligand types in the equatorial plane are consistent with a nearly square-planar complex of D_{4h} symmetry. Since $g_\parallel > g_\perp > 2.0$, a description of the electronic energy levels could be attempted assuming a $d_{x^2-y^2}$ ground state for the unpaired hole of the $3d^9$ Cu ion. The metal–ligand covalency, estimated from the following expression [20].

$$\alpha^2 = -\frac{a_\parallel}{P} + (g_\parallel - g_e) + \tfrac{3}{7}(g_\perp - g_e) + 0.04$$

P is the free-ion dipolar term (P = 0.036 cm^{-1}), g_e = 2.0023, $a_\parallel$ is taken to be negative, and α^2 was found to be 0.76. An approximate value of the transition energy level can be obtained if we replace the $g_\parallel$ value together with α^2 in $\Delta = -4\alpha^2\lambda/((g_\parallel/g_e) - 1)$, where λ is the spin-orbit constant for the free ion ($\lambda = -828$ cm^{-1}) [21]. A transition near 638 nm is predicted, consistent with the UV-Vis measurements. This confirms the d-d* character of the 620 nm transition. Other transitions in this frequency region are hidden by the broad 620 nm absorption band [22], preventing further interpretation. Nevertheless, by comparison of the small α^2 value with those of similar diketonate molecules, where it lies in the range $0.65 \leq \alpha^2 \leq 0.88$, significantly less than 1, it can be seen that the bond is quite covalent in nature and that the ligands are strongly bonded to the copper atom [22–24]. This low value of α^2 is also linked to the low $a_\parallel$ value. By comparison with the general values for a rigidly

square-planar complex and together with the position at the border of the Peisach-Blumberg plot, it has been shown that an increased $g_{\|}$ together with a decreased $a_{\|}$ originates from a weak tetrahedral distortion [25,26].

A third signal, C, associated with a copper dimer was also observed (see Fig. 6). On the basis of the same interpretation of the C signal as previously reported [27,28], an estimation of the $d_{\perp}$ component of the dimeric part of the spectrum was made. $d_{\perp}$ is defined as $d_{\perp} = D/g^{d}{}_{\perp}\mu_B$, where $g^{d}{}_{\perp} = 2.064$ and μ_B is the Bohr magneton, and D the zero-field splitting constant, itself defined through the electron-electron interaction Hamiltonian below (assuming axial symmetry).

$$H_{ee} = D\left(S_z^2 - \frac{S(S+1)}{3}\right)$$

$d_{\perp}$ was estimated to be 560 Gauss, leading to $D = 10.7 \cdot 10^{-25}$ J. Assuming that $g_{\|}$ is ca. 2.2, the Cu–Cu distance obtained through the relation below was $r \approx 4$ Å.

$$2D = \frac{\left(2g_{\|}^2 + g_{\perp}^2\right)\mu_B^2}{r^3}$$

This is reasonable for a face-to-face bimolecular association.

3.4.2. [CoL^3]

No ESR signal was obtained at room temperature for the cobalt complex. However upon cooling to liquid helium temperature a signal spread over nearly 6000 Gauss (0.6 Tesla) and showing g anisotropy was detected. The spectrum recorded at 4.2 K is reproduced in Fig. 7 where the g-tensor parameters are $g_1 = 5.42$, $g_2 = 3.67$ and $g_3 = 2.09$. The general shape of the spectrum, in particular the existence of g_i values very different from the free-electron value $g_e = 2.0023$, and the lack of signal at 300 K due to fast relaxation times, strongly suggest a high-spin Co^{II} complex [29–31]. The observed rhombicity in the g values is linked to the high sensitivity of any weak distortion of the ligand field in the case of the Co^{II} ion [32]. This alone does not permit determination of the symmetry of the cobalt sites [33,34]. One clue might be the broadness of the g_1-centred feature in the ESR spectrum, which is more indicative of (distorted) octahedral symmetry. Indeed, it has been shown that unresolved hyperfine structure is the major source of line broadening in high-spin Co complexes [35]. Since hyperfine coupling constants are much smaller for tetrahedral than for (distorted) octahedral complexes, the former usually show a sharper peak at that position [30,35]. This can be confirmed through the optical data. Peaks (additional to the main bands given in Table 1) were detected in the visible region at 510 nm ($\log \varepsilon = 1.76$), 602 nm ($\log \varepsilon = 1.41$), 654 nm ($\log \varepsilon = 1.3$), with a shoulder at 546 nm. Such low values of the molar extinction coefficient are observed in distorted and undistorted octahedral or square planar complexes [34], as opposed to those measured for tetrahedral symmetry. These symmetries would be consistent with the general shape of the molecule, in particular with the local environment of the Co^{II} ion tetracoordinated with oxygen atoms.

Co^{II} (nuclear spin $I = 7/2$) is in a $3d^7$ electronic configuration associated with a ^4F spectroscopic term. In moderate octahedral crystal fields, the ^4F term splits into an orbital singlet $A_{2g}(F)$ and two triplets $T_{1g}(F)$ and $T_{2g}(F)$ states, $T_{1g}(F)$ being the ground state. Through axial distortion, the $T_{1g}(F)$ and $T_{2g}(F)$ split again (see Fig. 8) [36]. The $A_{2g}(T_{1g})$ state is the lowest since $(g_1, g_2) > g_3$ [37]. Spin-orbital interaction lifts the final ground-state degeneracy into two Kramer doublets [33]. The separation between the ground-state doublet and the first excited level is larger than the

Fig. 7. ESR spectrum of the cobalt(II) complex in chloroform at 4.2 K.

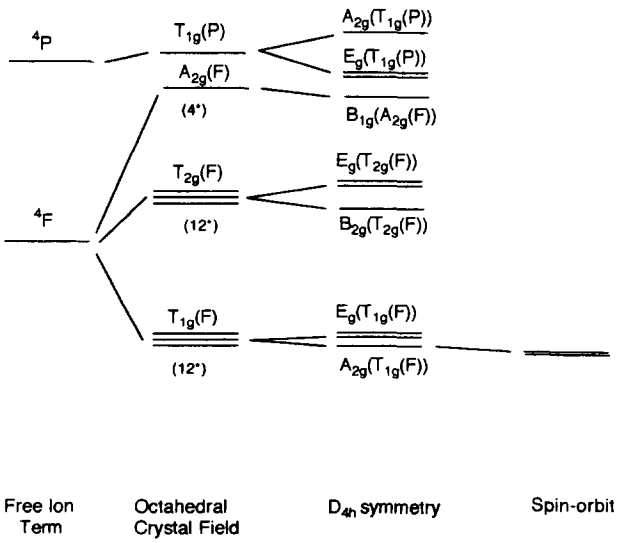

Fig. 8. Energy levels for a $3d^7$ ion in D_{4h} symmetry (the relative ordering of the levels $E_g(T_{1g}(P))/A_{2g}(T_{1g}(P))$ and $E_g(T_{1g}(F))/A_{2g}(T_{1g}(F))$ is arbitrary). * is the total degeneracy.

energy of the microwave source, leading to a $S = 1/2$ effective spin Hamiltonian.

The electronic spectra of (distorted) octahedral Co^{II} complexes show two main bands, one transition occurring in the 950–1540 nm range and the other in the 460–660 nm range [34]. They correspond to the $T_{1g}(F)$–$T_{2g}(F)$ and $T_{1g}(F)$–$A_{2g}(F)$ transitions, respectively. No near-IR measurements were made on our compounds. However the $T_{1g}(F)$–$T_{2g}(F)$ transition was calculated to be 7134 cm^{-1} [38]. Only the 654 nm transition was detected by UV-Vis measurements. It was assigned to the $A_{2g}(T_{1g})$–$B_{1g}(A_{2g}(F))$, since it is the lowest energetically, and also because it is the usually weak ($\log \varepsilon = 1.3$) [34]. The two transitions would be $A_{2g}(T_{1g})$–$E_g(T_{1g}(P))$ and $A_{2g}(T_{1g})$–$A_{2g}(T_{1g}(P))$ for the 602 and 510 nm, but here no assignment can be made since it is not possible to determine whether $E_g(T_{1g}(P))$ or $A_{2g}(T_{1g}(P))$ is higher.

According to Pilbrow [33], even for highly distorted octahedral complexes, one often finds $\langle g \rangle = 4.3$. In our case $\langle g \rangle = 3.7$. If we assumed a tetragonal distortion, the mean g-value could be expressed through the formula $\langle g \rangle = 10/3 + k$ where k is the orbital reduction factor, and any deviation of k from 1 (with $k \leq 1$) would be covalent in origin [39]. In this case k is 0.4, indicating a marked covalent character of the ligand–metal bond.

According to the local symmetry around the Co^{II} ion, one would expect a strictly square-planar complex with D_{4h} symmetry. Such compounds usually exist in a low-spin state [31–33]. The lowering of the symmetry observed here is associated with the extreme sensitivity of the Co^{II} ion to its environment. Regarding the rhombic character of the ESR spectrum and the number of optical transitions observed, distortion from octahedral or square-planar symmetry can be presumed [37]. Deviations from these ideal symmetries might come either from a weak tetrahedral distortion in the basal plane, or a tetragonal distortion of the octahedron. They can result from complexation with solvent molecules in the axial position, which possibility cannot be ignored or from the formation of oligomers. This latter possibility has already been invoked for similar complexes [14b].

4. Conclusions

This study established that the two-electron reduction mechanism of **3** is similar to that of **1** and **2**. As in **1** and **2**, the irreversible reduction of **3** occurred at the carbonyl groups and it was followed by an irreversible chemical reaction, which corresponded to a dehydrogenation of the primary electrochemical reduction products, i.e. $(H_2L^3)^{-\bullet}$ and $(H_2L^3)^{2-}$ leading ultimately to the enolate anion species $[L^3]^{2-}$. However, as expected from the electron-withdrawing effect of the pyrazolone group in **3**, the reduction of **3** occurred at potentials less negative than for **1** and **2**, and the dehydrogenation of the primary reduction products of **3** was extremely rapid. This behaviour may be ascribed to the greater acidicity of 4-acylpyrazolone-5 (pKa ~ 5) compared to that of β-diketones **1** and **2**.

Advantage has been taken of the characterization of the enolate anion $(L^3)^{2-}$ to prepare complexes $[ML^3]$ with facility and simply. Their identification and characterization were achieved by electrochemical and spectroscopic methods.

Electron paramagnetic resonance studies were carried out on the Co^{II} and Cu^{II} complexes and their magnetic parameters obtained. For $[CuL^3]$ a weakly tetrahedrally distorted square-planar symmetry was found, whereas for $[CoL^3]$ a distorted octahedron was proposed.

Further work directed towards the generalization of this electrosynthetic pathway to complexes of other bis(acyl-4-pyrazolones-5) is in progress.

References

[1] A. Kuncaka, A. Louati, M. Gross, C. Haubtmann, M. Bernard, J.J. André, Y. Frère and J.P. Brunette, *J. Chem. Soc., Faraday Trans., 89* (1993) 4299.

[2] X. Dong, F. Liu and Y. Zhao, *Huaxue Xuebao, 41* (1983) 848.

[3] S. Miyazaki, H. Mukai, S. Umetani, S. Kihara and M. Matsui, *Inorg. Chem., 28* (1989) 3014, and references therein.

[4] A. Tayeb, G.J. Goetz-Grandmont and J.P. Brunette, *Monats. für Chemie, 122* (1991) 453.

[5] B.S. Jensen, Acta Chem. Scand., 13 (1959) 1347.

[6] J. Bard, *Pure Appl. Chem., 25* (1971) 379, and references therein.

[7] M. Gross and J. Jordan, *J. Electroanal. Chem., Interfacial Electrochem., 75* (1977) 163.

[8] R.S. Nicholson and I. Shain, *Anal. Chem., 36* (1964) 706.

[9] J.N. Burnett, L.K. Hiller Jr. and R.W. Murray, *J. Electrochem. Soc., 117* (1970) 1028.

[10] N.L. Bauld and M.S. Brown, *J. Am. Chem. Soc., 89* (1967) 5413.

[11] A. Kuncaka, A. Louati, Y. Frère and M. Gross, *J. Electroanal. Chem., Interfacial Electrochem., 338* (1992) 213.

[12] E.C. Okafor, *Spectrochim. Acta, 37A* (1981) 939.

[13] K. Sone, *J. Am. Chem. Soc., 75* (1953) 5207.

[14] (a) F.A. Cotton and R.H. Holm, *J. Am. Chem. Soc., 82* (1960) 2979; (b) F.A. Cotton and R.H. Soderberg, *Inorg. Chem., 3* (1964) 1.

[15] H.B. Gray, in R.L. Carlin and M. Dekkar (eds.), *Transition Metal Chemistry*, Vol. 1, p. 239, New York, 1965, and references therein.

[16] E.C. Okafor, *Spectrochim. Acta, 37A* (1981) 945.

[17] K. Nakamoto, *Infrared Spectra of Inorganic and Coordination Compounds*, Wiley-Interscience, London, 1970, pp. 247–256.

[18] J.R. Ferraro, *Low-Frequency Vibrations of Inorganic and Coordination Compounds*, Plenum, New York, 1971, pp. 89–95.

[19] J. Peisach and W.E. Blumberg, *Arch. Biochem. Biophys., 165* (1974) 691.

[20] D. Kivelson and R. Neiman, *J. Chem. Phys., 35* (1961) 149.

[21] H.R. Gersmann and J.D. Swalen, *J. Chem. Phys., 36* (1962) 3221.

[22] H. Yokoi and T. Kishi, *Chem. Lett.*, (1973) 749.

[23] E.R. Menzel, D.R. Lorenz, J.R. Wasson, K.R. Radigan and B.J. McCormick, *J. Inorg. Nucl. Chem., 38* (1976) 993.
[24] S. Antosik, N.M.D. Brown, A.A. MacConnell and A.L. Porte, *J. Chem. Soc. A, 36* (1969) 545.
[25] U. Sakaguchi and A.W. Addison, *J. Chem. Soc., Dalton Trans.*, (1979) 606.
[26] E.G. Seebauer, E.P. Duliba, D.A. Scogin, R.B. Gennis and R.L. Belford, *J. Am. Chem. Soc., 105* (1983) 4926.
[27] A. Aboukaïs, R. Bechara, D. Ghoussoub, C.F. Aïssi, M. Guelton and J.P. Bonnelle, *J. Chem. Soc., Faraday Trans.*, (1991) 87, 631.
[28] A. Aboukaïs, A. Bennani, C.F. Aïssi, G. Wrobel, M. Guelton and J.C. Vedrine, *J. Chem. Soc., Faraday Trans., 88* (1992) 615.
[29] J. Zarembovitch and O. Kahn, *Inorg. Chem., 23* (1984) 589.
[30] A. Bencini, I. Bertini, G. Canti, D. Gatteschi and C. Luchinat, *J. Inorg. Biochem., 14* (1981) 8193.
[31] F.E. Mabbs and D. Collison, *Electron Paramagnetic Resonance of d Transition Metal Compounds,* Elsevier, Amsterdam, 1992.
[32] A. Abragam and B. Bleaney, *Electron Paramagnetic Resonance of Transition Ions,* Clarendon, Oxford, 1970, p. 449.
[33] J.R. Pilbrow, *Transition Ion Electron Paramagnetic Resonance,* Clarendon, Oxford, 1990, p. 10 and p. 149.
[34] L. Banci, A. Bencini, C. Benelli, D. Gatteschi, C. Zanchini, *Struct. Bonding (Berlin), 52* (1992) 37.
[35] S.A. Cockle, S. Lindskog and E. Grell, *Biochem. J., 143* (1974) 703.
[36] A. Abragam and M.H.L. Pryce, *Proc. Roy. Soc., A206* (1951) 173.
[37] A. Bencini, C. Benelli, D. Gatteschi and C. Zanchini, *Inorg. Chem., 19* (1980) 1301.
[38] E. König, *Struct. Bonding (Berlin), 9* (1971) 175.
[39] M. Tinkham, *Proc. Roy. Soc., A236* (1956) 544.